

# Synchronization Phenomena in Chaotic Circuits in Unidirectional Coupling

Kohei Suzue, Yoko Uwate and Yoshifumi Nishio

Dept. of Electrical and Electronic Engineering, Tokushima University  
2-1 Minami-Josanjima, Tokushima 770-8506, Japan

Email: [c612001195@tokushima-u.ac.jp](mailto:c612001195@tokushima-u.ac.jp) , [uwate@ee.tokushima-u.ac.jp](mailto:uwate@ee.tokushima-u.ac.jp) , [nishio@ee.tokushima-u.ac.jp](mailto:nishio@ee.tokushima-u.ac.jp)

**Abstract**—In this study, we investigate the variation of synchronization phenomena with the coupling strength between the circuits when the chaotic circuits, called Nishio-Inaba circuits, are coupled in a unidirectional manner. As a result, when the coupling strength is equal in two pairs, the synchronization rate is higher in the pair with equal parameters. On the other hand, when the coupling strength of the pair with different parameters was twice that of the pair with the same parameters, the synchronization rate of the two pairs became equal from a certain value.

## I. INTRODUCTION

Synchronization phenomena are numerous in nature. This phenomenon is exemplified by the metronome and the collective firing of neurons, the nerve cells of the brain. In recent years, research on AI(Artificial Intelligence) has been conducted extensively, and a variety of high-performance AI products have been commercialized. However, current AI uses linear circuit models to generate images and sort out similar information, whereas we humans actually use nonlinear and aperiodic signals. Therefore, we believe that we can make AI more similar to the human brain by using chaotic circuits that have the same characteristics as biological signals. In this study, we investigate the synchronization phenomenon of chaotic circuits as a basic research. The chaotic circuit used in this study is the Nishio-Inaba circuit published in 1989 [1].

In a previous study, the synchronization phenomenon of chaotic circuits in networks coupled by unidirectional coupling was investigated using a chaotic circuit different from the Nishio-Inaba circuit [2][3]. In that study, synchronization phenomena of unidirectional chaotic circuits coupled in other than ring topology were investigated.

In this study, the synchronization phenomena of chaotic circuits connected by unidirectional coupling from two chaotic circuits were investigated using the Nishio-Inaba circuit. In order to investigate the synchronization phenomena in more detail, three nodes were used to investigate the synchronization phenomena with each node in the case where one node is affected by two nodes. The synchronization rates at each parameter were investigated when the coupling strength between the circuits was varied.

## II. CIRCUIT AND SYSTEM MODEL

Figure 1 shows a schematic of the Nishio-Inaba circuit used in this study.

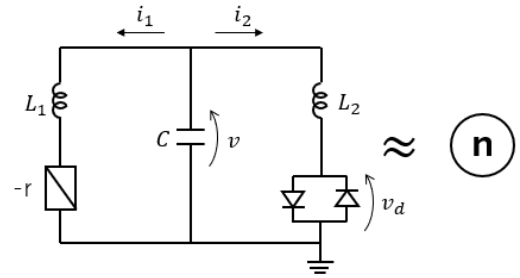


Fig. 1. Circuit Model.

The circuit equations in Fig. 1 are given as follows:

$$\begin{cases} L_1 \frac{di_1}{d\tau} = v + ri_1, \\ L_2 \frac{di_2}{d\tau} = v - v_d, \\ C \frac{dv}{d\tau} = -i_1 - i_2 \end{cases} \quad (1)$$

For Eq. (1)  $v_d$  represents the voltage at the diode portion of Fig. 1, and its characteristic equation is defined as follows:

$$v_d = \frac{r_d}{2} \left( \left| i_2 + \frac{V}{r_d} \right| - \left| i_2 - \frac{V}{r_d} \right| \right) \quad (2)$$

The normalization parameters for normalizing Eq. (1) are as follows:

$$\begin{aligned} i_1 &= \sqrt{\frac{C}{L_1}} V x_n, & i_2 &= \frac{\sqrt{L_1 C}}{L_2} V y_n, & v &= V z_n, \\ \alpha &= r \sqrt{\frac{C}{L_1}}, & \beta &= \frac{L_1}{L_2}, & \delta &= r_d \frac{\sqrt{L_1 C}}{L_2}, \\ \gamma &= \frac{1}{R}, & t &= \sqrt{L_1 C} \tau, & \text{"."} &= \frac{d}{d\tau} \end{aligned}$$

The normalized equation for this circuit is given as Eq. (3).

$$\begin{cases} \dot{x}_i = \alpha x_i + z_i, \\ \dot{y}_i = z_i - f(y_i), \\ \dot{z}_i = -x_i - \beta y_i - \sum_{i,j=0}^n \gamma_{ij}(z_i - z_j), \\ f(y_i) = \frac{\delta}{2} (|y_i + \frac{1}{\delta}| - |y_i - \frac{1}{\delta}|) \end{cases} \quad (3)$$

Figure 2 shows the model of the system used in this study. In this figure, a single Nishio-Inaba circuit is defined as a single node.

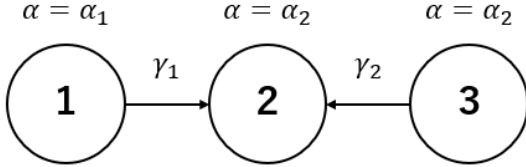


Fig. 2. System Model.

In this study, the value of  $\alpha$  a parameter indicating the degree of chaos in the system shown in Fig. 2, is set as follows.

- Case1.  $\alpha_1 = 0.425, \alpha_2 = 0.415$   
Case2.  $\alpha_1 = 0.420, \alpha_2 = 0.410$   
Case3.  $\alpha_1 = 0.425, \alpha_2 = 0.405$   
Case4.  $\alpha_1 = 0.430, \alpha_2 = 0.400$

In this system, the ratio of coupling strength  $\gamma_1$  to  $\gamma_2$  was initially set to 1:1. Next, the ratio of coupling strength  $\gamma_1$  to  $\gamma_2$  was set to 2:1. Then, the value of coupling strength  $\gamma_1$  was varied from 0 3.0 in 0.5 increments, and where a more detailed value was desired, it was varied in 0.1 increments. The synchronization rate of the pair of chaotic circuits used in each of these couplings was measured using Eq. (4).

To increase the reliability of the data, the results are varied in five different initial values and the average of these values is taken.

$$S_i = \frac{count_{syn_i}}{count_{all}} \times 100 \quad (4)$$

In Eq. (4),  $S_i$  is defined as the synchronization rate between node 2 and node  $i$ ,  $count_{syn_i}$  is the number of counts in which node 2 and node  $i$  were synchronized, and  $count_{all}$  is all counts.

In measuring the synchronization rate, we compared the value of  $z$  in Eq. (3) for each chaotic circuit; we counted cases where the absolute difference in the value of  $z$  for a pair of chaotic circuits was smaller than 0.1, and measured the synchronization rate by finding the percentage from the total counts.

However, one count is defined as the solution of the circuit equation by the Runge-Kutta method on the simulation.

### III. SIMULATION RESULTS

In this section, we describe the change in the synchronization rate for each value of  $\alpha$  when the ratio of coupling strengths is changed.

In this study, parameters other than  $\alpha$  in the chaotic circuit were set to values of  $\beta = 3.0$  and  $\delta = 470$ . The counts were taken as all counts from 40000 to 100000 counts, except for counts 0 to 39999 counts, which were expected to be transient.

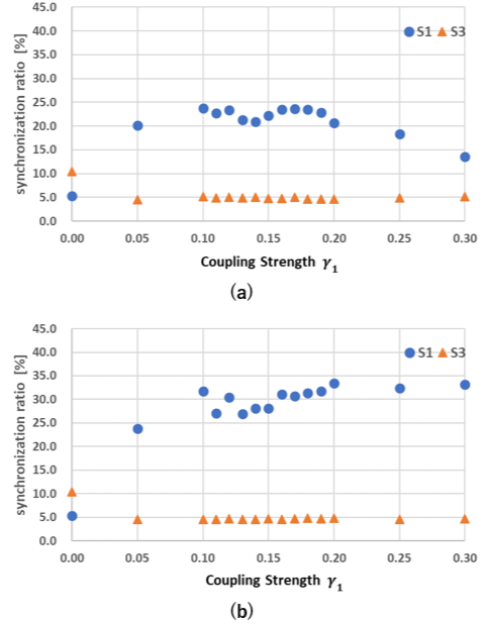


Fig. 3. Case 1 ((a)  $\gamma_1 : \gamma_2 = 1 : 1$  (b)  $\gamma_1 : \gamma_2 = 2 : 1$ ).

Figure 3 shows the simulation results of Case 1: in Case 1, node 1 is the chaotic solution, and the other nodes have 3-period solutions. Therefore, node 2 contains the chaotic solution, and  $S_1$  is higher regardless of the ratio of the coupling strength. Furthermore,  $S_3$  is less than 10 in almost all cases.

Figure 4 shows the simulation results for Case 2; in Case 2, all nodes have chaotic solutions. In the case of the ratio of coupling strength of 1:1, it can be seen that  $S_3$  is more than 5% larger than  $S_1$  because the parameters are the same. In the case of the ratio of coupling strength of 2:1,  $S_3$ , which is the synchronization rate between node 3 and node 2 with the same parameters, is larger at low values of coupling strength, but as the coupling strength increases,  $S_1$  and  $S_3$  become equal. Further increasing the coupling strength,  $S_1$  becomes larger than  $S_3$ .

Figure 5 shows the simulation results for Case 3; in Case 3, all nodes have chaotic solutions. In the case of the ratio of coupling strength of 1:1, it can be seen that  $S_3$  is more than 10% larger than  $S_1$  because the parameters are the same. In the case of the ratio of coupling strength of 2:1,  $S_3$  is larger

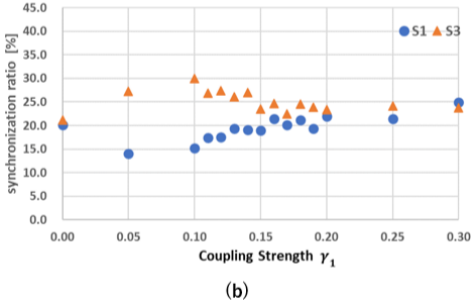
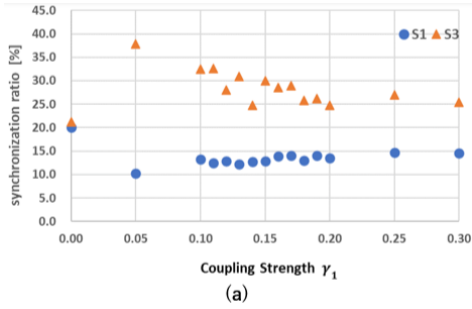


Fig. 4. Case 2 ((a)  $\gamma_1 : \gamma_2 = 1 : 1$  (b)  $\gamma_1 : \gamma_2 = 2 : 1$ ).

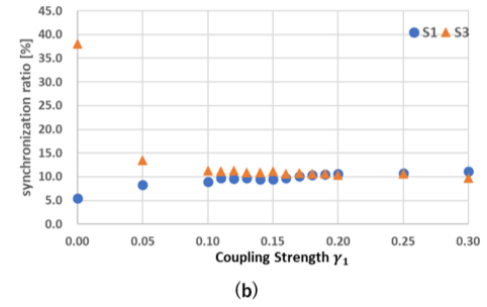
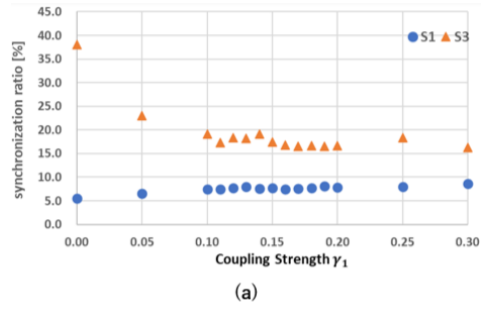


Fig. 6. Case 4 ((a)  $\gamma_1 : \gamma_2 = 1 : 1$  (b)  $\gamma_1 : \gamma_2 = 2 : 1$ ).

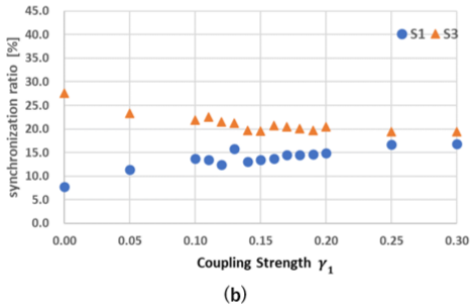
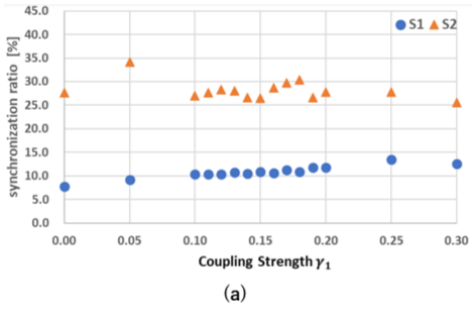


Fig. 5. Case 3 ((a)  $\gamma_1 : \gamma_2 = 1 : 1$  (b)  $\gamma_1 : \gamma_2 = 2 : 1$ ).

for lower values of coupling strength because the parameters are the same, but as the coupling strength increases, the synchronization rate approaches the same value.

Figure 6 shows the simulation results for Case 4; in Case 4, all nodes have chaotic solutions. In the case of the ratio of coupling strength of 1:1, it can be seen that  $S_3$  is more than 5% larger than  $S_1$  because the parameters are the same. In the case of the ratio of coupling strengths of 2:1, the synchronization rate has the same value if the value of the coupling strength  $\gamma_1$  is greater than 0.1. When the coupling strength  $\gamma_1$  is greater

than 0.17,  $S_1$  is greater than  $S_3$ .

#### IV. CONCLUSIONS

In this study, the Nishio-Inaba circuit was used to investigate the synchronization rate when chaotic circuits are unidirectionally coupled. First, for the same coupling strength, the synchronization rate was higher for pairs with the same parameters unless the solution of the chaotic circuit was a 3-period solution. Second, when the coupling strength of pairs with different parameters was doubled, the synchronization rate was higher for pairs with the same parameters as in the same coupling strength case while the coupling strength was small. However, as the coupling strength increased, the synchronization rate remained constant regardless of the parameters. In the future, we would like to investigate how the synchronization rate changes with coupling strength by changing various parameters.

#### REFERENCES

- [1] Yoshifumi Nishio, Naohiko Inaba, Shinsaku Mori, Toshimichi Saito, "Rigorous Analyses of Windows in a Symmetric Circuit", IEEE International Symposium on Circuits and Systems, vol. 3, pp. 2151-2154, May 1989.
- [2] Akari Oura, Kyohei Fujii, Yoko Uwate, Yoshifumi Nishio, "Analysis of Chaotic Circuit Networks with One-Way Coupling", International SoC Design Conference, pp. 168-169, Nov. 2018.
- [3] Yuki Matsubara, Yuki Ishikawa, Yoko Uwate, Yoshifumi Nishio, "Synchronization of Bi-Directionally Coupled Chaotic Circuits with Non-Uniform Coupling Strength", RISP International Workshop on Nonlinear Circuits, Communications and Signal Processing, pp. 154-157, Feb. 2023.